

## Gallium Cluster “Magic Melters”

Gary A. Breaux, Damon A. Hillman, Colleen M. Neal, Robert C. Benirschke, and Martin F. Jarrold\*

Chemistry Department, Indiana University, 800 East Kirkwood Avenue, Bloomington, Indiana 47405-7102

Received April 19, 2004; E-mail: mfj@indiana.edu

It is now well established that the melting points for particles with thousands of atoms decrease with the particle size. This melting point depression, which is due to the change in the surface-to-volume ratio, scales approximately with the inverse of the radius ( $1/r$ ).<sup>1–7</sup> In the cluster size regime,  $<500$  atoms, the thermodynamic scaling responsible for the  $1/r$  dependence breaks down and size-dependent fluctuations in the melting transitions are expected. Much less is known about the melting behavior in this size regime. The pioneering studies of Haberland and collaborators<sup>8–11</sup> on sodium clusters have provided most of what we know from an experimental stand point. However, the factors that contribute to the size-dependent melting behavior remain poorly understood.

In the work reported here we have used calorimetry measurements to probe the melting of unsupported gallium clusters,  $\text{Ga}_n^+$  with  $n = 30–50$  and  $55$ . The results show a remarkably strong dependence on cluster size. For some clusters no melting transition is observed, while others (the “magic melters”) have particularly well-defined melting transitions. The addition or removal of a single atom can make an enormous difference, even changing a nonmelter to a magic melter. There is a strong correlation between the heats of fusion and the relative stabilities of the clusters. However, these quantities are not strongly correlated with the melting temperatures.

The calorimetry measurements were performed using a method based on multicollision-induced dissociation.<sup>12</sup> Cluster ions are created in a laser ablation source with a liquid metal target, and their temperature is set in a 15 cm long extension that is adjustable from 77 to 1200 K. After exiting the extension, a specific cluster size is selected with a quadrupole mass spectrometer, accelerated, and focused into a collision cell that contains 1 Torr of helium. As the ions enter the collision cell, they are heated by numerous collisions with the buffer gas, and some of them fragment. They dissociate by sequential atom loss. The parent and fragment ions are analyzed by a second quadrupole mass spectrometer and then detected. The amount of fragmentation is monitored as a function of the ions’ translational energy (TE) as they enter the collision cell, and the TE for 50% dissociation (TE50%D) is determined from a linear regression. TE50%D values are then measured as a function of the temperature of the extension. The TE50%D values become smaller as the temperature is raised because the cluster’s internal energy increases. The derivative of TE50%D with respect to temperature is approximately proportional to the heat capacity of the cluster. The proportionality constant relates a change in the cluster’s internal energy to a change in the TE. A simple impulsive collision model<sup>13</sup> provides a good estimate of the proportionality constant (the resulting heat capacities are in good agreement with the expected values).

Figure 1 shows plots of the heat capacities determined as a function of temperature for  $\text{Ga}_n^+$  with  $n = 30–50$  and  $55$ . The points are the measured values, and the dashed lines are heat capacities derived using statistical thermodynamics with a modified Debye model, which incorporates a low-frequency cutoff to account for the cluster’s finite size.<sup>14</sup> The melting point of a bulk material

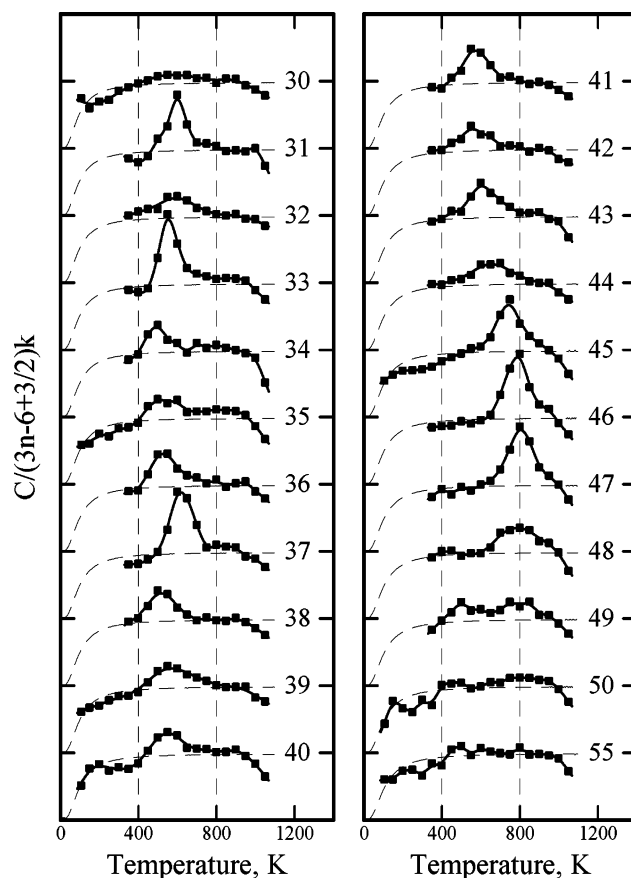


**Figure 1.** Heat capacities plotted against temperature for  $\text{Ga}_n^+$  with  $n = 30–50$  and  $55$ . The points are the measured values, and the dashed lines are calculated from statistical thermodynamics.  $(3n - 6 + 3/2)k$  is the classical (vibrational + rotational) heat capacity.

is indicated by a sharp spike (essentially a  $\delta$ -function) in the heat capacity due to the heat of fusion. For a finite-sized system, the spike in the heat capacity is expected to be broadened because the liquid and solid phases can coexist over a significant temperature range.<sup>15</sup> This broadening is clearly evident in Figure 1 where the transitions are 200–300 K wide. The studies described here were performed with ions, but the presence of the charge is not expected to significantly perturb the melting transition.<sup>16</sup>

Melting transitions are observed for most of the clusters in Figure 1 at between 500 and 800 K. Note that particularly well-defined transitions are observed for clusters with  $n = 31, 33, 37,$  and  $45–47$  (the “magic melters”). For some clusters, no obvious melting transition is observed ( $n = 30, 50,$  and  $55$ ), while others have small, poorly defined melting transitions ( $n = 32, 34, 44,$  and  $49$ ). For  $\text{Ga}_{30}^+$  to  $\text{Ga}_{33}^+$ , the addition or subtraction of a single atom causes oscillations between a well-defined melting transition and no melting transition or a poorly defined transition.  $\text{Ga}_{45}^+, \text{Ga}_{46}^+,$  and  $\text{Ga}_{47}^+$  have well-defined melting transitions. Between  $\text{Ga}_{47}^+$  and

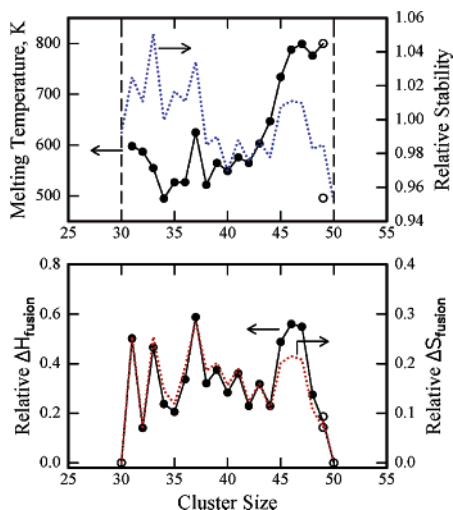


**Figure 2.** Melting temperatures, cluster relative stabilities, relative heats of fusion, and relative entropies of fusion plotted against cluster size. The dashed vertical lines represent clusters where no melting transition is observed. Two points are shown for  $\text{Ga}_{49}^+$  to represent the two peaks in the heat capacities for this cluster.

$\text{Ga}_{49}^+$ , the melting transition rapidly diminishes, and it apparently disappears at  $\text{Ga}_{50}^+$ .

$\text{Ga}_{49}^+$  has two small maxima in its heat capacity plot, at around 500 and 800 K. These features are reproducible. The heat capacity plots for  $\text{Ga}_{50}^+$  and  $\text{Ga}_{55}^+$  have shoulders at around 400 K. These features are also reproducible. The shoulders may result from melting transitions without a significant latent heat, the shoulder then represents the small jump in the heat capacity expected on going from a solid to a liquid cluster. If this is the case, the shoulders for  $\text{Ga}_{50}^+$  and  $\text{Ga}_{55}^+$  may be related to the lower temperature maximum in the heat capacity plot for  $\text{Ga}_{49}^+$ . We studied the 55 atom cluster because it may form a Mackay icosahedron, which is expected to have a well-defined melting transition. This is clearly not the case for  $\text{Ga}_{55}^+$ .

It is evident from Figure 1 that there are systematic drops in the heat capacities for all clusters at  $>1000$  K. This probably results from the emission of blackbody radiation as the clusters travel from the extension (where their temperature is set) to the collision cell. This emission will lower the internal energy of the hot clusters and make it appear that they have reduced heat capacities. Cooling by spontaneous atom evaporation can be ruled out.

Figure 2 shows the melting temperatures (from the centers of the spikes in the heat capacities), the cluster relative stabilities, the relative heats of fusion, and the relative entropies of fusion plotted against cluster size. The relative heats of fusion were obtained by integrating the areas under the spikes in the heat capacities and dividing by  $n$  times the bulk heat of fusion,  $5.59 \text{ kJ mol}^{-1}$ . The entropies of fusion were obtained from  $\Delta S_{\text{fusion}} = \Delta H_{\text{fusion}}/T_{\text{melt}}$  and then divided by the bulk value. The cluster relative stabilities were estimated from the TE50%D values at 323 K (which is well below the melting transition) divided by the number of atoms in the cluster. Note in Figure 2 the large variations in the melting temperatures, including the 200 K jump between  $\text{Ga}_{42}^+$  and  $\text{Ga}_{46}^+$ , the magic melters with large relative heats of fusion (50–60% of the bulk

value) at  $n = 31, 33, 37,$  and  $45-47$ , and the clear pattern of odd–even oscillations in the cluster relative stabilities.

The clusters that melt do so substantially (200–500 K) above the bulk melting point of 303 K. Melting temperatures above the bulk value have previously been observed for small tin clusters<sup>17</sup> and attributed to the clusters having geometries that are different from the bulk.<sup>18</sup> Presumably, the high melting temperatures for the gallium clusters also result from geometries that are different from the bulk. The step in the melting temperatures at  $\text{Ga}_{42}^+$  to  $\text{Ga}_{46}^+$  may reflect a geometry change.

The only other system where melting points have been recorded in the cluster size regime ( $<500$  atoms) is for sodium. A number of  $\text{Na}_n^+$  clusters with 40–350 atoms have been studied.<sup>10,11</sup> Most  $\text{Na}_n^+$  clusters with  $<90$  atoms do not show a clear melting transition. The melting temperatures for those that do melt are all below the bulk value, and the size-dependent fluctuations in the melting temperatures ( $<100$  K) are much smaller than for gallium.

For the gallium clusters, there is a strong correlation between the heats of fusion, the entropies of fusion, and the cluster relative stabilities (see Figure 2). The correlation between the heats of fusion and the relative stabilities presumably results because more energy is required to melt the more strongly bound clusters. A strong correlation between the enthalpies and entropies of fusion appears to be a common phenomenon (it has also been observed for  $\text{Na}_n^+$  clusters).<sup>11,19</sup> This enthalpy/entropy compensation reduces the fluctuations in the melting temperatures (because  $T_{\text{melt}} = \Delta H_{\text{fusion}}/\Delta S_{\text{fusion}}$ ) and this is why the melting temperatures are not correlated with the cluster relative stabilities. The origin of the enthalpy/entropy compensation is not easily explained.<sup>19</sup> In the present case, the correlation may be between  $\Delta S_{\text{fusion}}$  and the stabilities of the clusters; such a correlation may result because the strongly bound clusters are more ordered and more rigid.

**Acknowledgment.** We gratefully acknowledge the support of the National Science Foundation.

## References

- (1) Pawlow, P. *Z. Phys. Chem.* **1909**, *65*, 1–35.
- (2) Couchman, P. R.; Jesser, W. A. *Nature (London)* **1977**, *269*, 481–483.
- (3) Takagi, M. *J. Phys. Soc. Jpn.* **1954**, *9*, 359–363.
- (4) Buffat, Ph.; Borell, J. P. *Phys. Rev. A* **1976**, *13*, 2287–2298.
- (5) Hoshino, K.; Shimamura, S. *Philos. Mag. A* **1979**, *40*, 137–141.
- (6) Peppiatt, S. J. *Proc. R. Soc. (London) A* **1975**, *345*, 401–412.
- (7) Lai, S. L.; Guo, J. Y.; Petrova, V.; Ramanath, G.; Allen, L. H. *Phys. Rev. Lett.* **1996**, *77*, 99–102.
- (8) Schmidt, M.; Kusche, R.; Kronmüller, W.; von Issendorf, B.; Haberland, H. *Phys. Rev. Lett.* **1997**, *79*, 99–102.
- (9) Schmidt, M.; Kusche, R.; von Issendorf, B.; Haberland, H. *Nature (London)* **1998**, *393*, 238–240.
- (10) Schmidt, M.; Haberland, H. C. *R. Physique* **2002**, *3*, 327–340.
- (11) Schmidt, M.; Donges, J.; Hippler, Th.; Haberland, H. *Phys. Rev. Lett.* **2003**, *90*, 103401.
- (12) Breaux, G. A.; Benirschke, R. C.; Sugai, T.; Kinnear, B. S.; Jarrold, M. F. *Phys. Rev. Lett.* **2003**, *91*, 215508.
- (13) Jarrold, M. F.; Honea, E. C. *J. Phys. Chem.* **1991**, *95*, 9181–9185.
- (14) Bohr, J. *Int. J. Quantum Chem.* **2001**, *84*, 249–252.
- (15) Beck, T. L.; Jellinek, J.; Berry, R. S. *J. Chem. Phys.* **1987**, *87*, 545–554.
- (16) Calvo, F.; Spiegelman, R. *J. Chem. Phys.* **2000**, *112*, 2888–2908.
- (17) Shvartsburg, A. A.; Jarrold, M. F. *Phys. Rev. Lett.* **2000**, *85*, 2530–2532.
- (18) Joshi, K.; Kanhere, D. G.; Blundell, S. A. *Phys. Rev. B* **2003**, *67*, 235413.
- (19) Williams, D. H.; O'Brien, D. P.; Bardsley, B. *J. Am. Chem. Soc.* **2001**, *123*, 737–738.

JA0477423